

1 **The influence of heteroresistance on minimum inhibitory concentration (MIC),**
2 **investigated using weak-acid stress in food spoilage yeasts**

3

4 Joseph Violet¹, Joost Smid², Annemarie Pielaat², Jan-Willem Sanders² and Simon V. Avery^{1,*}

5

6 ¹School of Life Sciences, University of Nottingham,

7 Nottingham NG7 2RD, United Kingdom

8

9 ²Unilever Foods Innovation Centre,

10 Bronland 14, 6708 WH Wageningen, the Netherlands

11

12

13

14 **Running title:** Heteroresistance of spoilage yeasts to sorbic acid

15

16

17 **Key words:** cell individuality, inoculum effect, weak acid preservatives, food security, food spoilage,

18 phenotypic heterogeneity

19

20

21

22

23

24 ***Corresponding author:** Simon.Avery@nottingham.ac.uk

25 Abstract

26 Populations of microbial cells may resist environmental stress by maintaining a high population-
27 median resistance (IC_{50}) or, potentially, a high variability in resistance between individual cells
28 (heteroresistance); where heteroresistance would allow certain cells to resist high stress, provided
29 the population was sufficiently large to include resistant cells. This study sets out to test the
30 hypothesis that both IC_{50} and heteroresistance may contribute to conventional minimal-inhibitory-
31 concentration (MIC) determinations, using the example of spoilage-yeast resistance to the
32 preservative sorbic acid. Across a panel of 26 diverse yeast species, both heteroresistance and
33 particularly IC_{50} were positively correlated with predicted MIC. A focused panel of 29 different
34 isolates of a particular spoilage yeast was also examined (isolates previously recorded as
35 *Zygosaccharomyces bailii*, but genome resequencing revealing that several were in fact hybrid
36 species, *Z. parabailii* and *Z. pseudobailii*). Applying a novel high-throughput assay for
37 heteroresistance, it was found that IC_{50} but not heteroresistance was positively correlated with
38 predicted MIC when considered across all isolates of this panel, but the heteroresistance-MIC
39 interaction differed for the individual *Zygosaccharomyces* subspecies. *Z. pseudobailii* exhibited
40 higher heteroresistance than *Z. parabailii* whereas the reverse was true for IC_{50} , suggesting possible
41 alternative strategies for achieving high MIC between subspecies. This work highlights the limitations
42 of conventional MIC measurements due to the effect of heteroresistance in certain organisms, as
43 the measured resistance can vary markedly with population (inoculum) size.

44

45 Importance

46 Food spoilage by fungi is a leading cause of food waste, with specialised food spoilage yeasts capable
47 of growth at preservative concentrations above the legal limit, in part due to heteroresistance
48 allowing small subpopulations of cells to exhibit extreme preservative resistance. Whereas

49 heteroresistance has been characterised in numerous ecological contexts, measuring this phenotype
50 systematically and assessing its importance are not encompassed by conventional assay methods.
51 The development here of a high-throughput method for measuring heteroresistance, amenable to
52 automation, addresses this issue and has enabled characterisation of the contribution that
53 heteroresistance may make to conventional MIC measurements. We used the example of sorbic acid
54 heteroresistance in spoilage yeasts like *Zygosaccharomyces* spp, but the approach is relevant to
55 other fungi and other inhibitors, including antifungals. The work shows how median resistance,
56 heteroresistance and inoculum size should all be considered when selecting appropriate inhibitor
57 doses in real-world antimicrobial applications such as food preservation.

58

59 Introduction

60 Resistance of microorganisms to inhibitory agents is a growing problem in therapeutics (Andersson
61 et al., 2019, Dewachter et al., 2019) and food supply chains (Davies et al. 2020). The resistance of a
62 microorganism to a stressor is typically described using a conventional minimum inhibitory
63 concentration (MIC) measurement, which reflects the concentration of a stressor required to
64 prevent growth at a particular fixed inoculum size (Box 1). Other measures of stress resistance
65 include IC_{50} , a population-median measure describing the concentration required to inhibit either
66 50% of cells in a population (as used in the present work, Box 1) or all cells by 50%, depending on the
67 study. In recent years there has been growing recognition also of heteroresistance, describing the
68 heterogeneity of resistance between individual clonal cells (Box 1), which appears to be very
69 ubiquitous (Bishop et al. 2007, Holland et al. 2014, Jing et al. 2018, Levy et al., 2012). However, the
70 extent to which differences in heteroresistance may contribute to MIC of a cell inoculum remains
71 barely explored, especially relative to traditional measures such as IC_{50} . The present work aimed to
72 address this gap in our knowledge, as it could explain variability in MIC data that are used as
73 common standards, due to parameters such as population size and the inoculum effect (Box 1).

Box 1: Definitions of parameters

- 1) **MIC**: minimum inhibitory concentration, i.e., lowest concentration of a stressor required to completely inhibit the growth of an inoculum of a microorganism.
- 2) **MIC^{EXP}**: Experimentally derived MIC, at a given inoculum size, e.g., the MIC^{EXP} for 100 cells of a given strain could be different to the MIC^{EXP} for 10,000 cells of the same strain.
- 3) **MIC^{MODEL}**: MIC of 10,000 cells/well predicted using a lognormal distribution curve, fitted to MIC^{EXP} values (see *Fitting to normal and lognormal distributions*)
- 4) **Heteroresistance**: Cell-cell phenotypic heterogeneity in a resistance phenotype. Here quantified as the standard deviation of a lognormal distribution of single cell resistances
- 5) **IC₅₀**: Population-median resistance, here defined as the mean of a lognormal distribution of single cell resistances
- 6) **Inoculum effect**: Phenomenon by which MIC^{EXP} increases with inoculum size, due to increased probability of resistant cells being present

74

75 Phenotypic heterogeneity among individual cells of genetically uniform populations is considered an
76 evolutionarily selected strategy akin to bet hedging (Ackermann 2015). It describes cell-to-cell
77 variation in a phenotype (e.g. stress resistance) within a cell population, resulting in phenotypically
78 (not genotypically-) distinct subpopulations among which some may be better equipped to thrive if
79 conditions change (Ackermann 2015, Smith et al., 2007, Levy et al. 2012, Stratford et al 2019). The
80 rationale is that generation of phenotypic heterogeneity, may be a relatively low cost strategy
81 (metabolically) for improving survival-chances in uncertain conditions. Such heterogeneity in the
82 case of stress resistance can be observed in almost any resistance phenotype: examples of
83 heteroresistance are evident in microbial responses to antibiotics (Dewachter et al., 2019, Scheler et
84 al., 2020, Jing et al. 2018), heat (Levy et al., 2012), osmotic (Stratford et al. 2019), metal (Holland et
85 al., 2014) and weak organic acid (Stratford et al. 2014, Geoghegan et al. 2020) stresses. Mechanistic
86 determinants of heteroresistance have been characterised, including cell-to-cell variation in gene
87 expression linked to particular ‘high’ or ‘low’-variation promoters or transcription factors, commonly
88 referred to as gene expression noise (Silander et al. 2011, Urchueguia et al., 2021, Newman et al.
89 2006). Housekeeping genes tend to be expressed with low variation between cells, whereas high-
90 variation promoters are more commonly associated with stress-response genes (Newman et al.
91 2006). Engineering increased variation of expression of an oxidative stress response gene has been
92 shown to increase resistance to oxidative stress in *Saccharomyces cerevisiae* (Liu et al., 2018), while
93 dampening of expression variation in similar functions gave decreased resistance (Smith et al.,
94 2007).

95 As food spoilage microorganisms can exhibit both high population-median resistance and
96 heteroresistance to food preservatives (Stratford et al. 2014), they provide a good example with
97 which to address this study’s main aim to characterise the relationship between MIC and
98 heteroresistance versus population-median resistance. Among the major food preservatives, sorbic
99 acid is a weak organic acid preservative widely used in condiments and drinks of $\text{pH} \leq 4$, conditions in
100 which the acid is undissociated and capable of traversing the plasma membrane. Several modes of

101 action have been proposed for sorbic acid, including cytosolic acidification (Stratford et al., 2013a)
102 and disruption of the mitochondrial electron transport chain (Stratford et al., 2020). Efficacy of
103 sorbic acid as a food preservative is hampered by the intrinsic resistance of specialised spoilage
104 yeasts, which are capable of growth at sorbic concentrations exceeding the maximum legal limit
105 dictated by food standards agencies (Stratford et al., 2013b).

106 *Zygosaccharomyces bailii* is a food spoilage yeast exhibiting a high level of resistance to weak organic
107 acids (Stratford et al. 2014). Two interspecies hybrids related to *Z. bailii* and also reported to spoil
108 preserved foods are *Z. parabailii* and *Z. pseudobailii*, formed through hybridisation events between
109 ancestral *Z. bailii* and two unknown *Zygosaccharomyces* species, sharing approximately 90-93%
110 sequence identity with *Z. bailii* (Braun-Galleani et al., 2018). *Z. bailii* has several proposed
111 mechanisms of resistance to weak organic acids, including a relatively thick and rigid plasma
112 membrane (Lindberg et al. 2013, Lindahl et al. 2016), metabolism of sorbic acid to less inhibitory
113 products (Mollapour and Piper, 2001), metabolism that is primarily fermentative (Stratford et al.
114 2020) and a low cytosolic pH (Stratford et al. 2013b, 2014). In addition to being relatively resistant to
115 sorbic acid (according to MIC or IC₅₀), *Z. bailii* also shows high sorbic acid heteroresistance (Stratford
116 et al. 2013b), with a small proportion of cells capable of resisting extreme concentrations even
117 though they may take several weeks to grow to detectable levels.

118 The food-industry relevance of *Z. bailii*, coupled with its high heteroresistance makes it an ideal
119 model for studying the relative contributions of population-median resistance and heteroresistance
120 to MIC. In this study we assess and compare these parameters in a panel of diverse spoilage yeasts
121 as well as more select panels of *Z. bailii*, *Z. parabailii* and *Z. pseudobailii* isolates. The work highlights
122 the importance of context when assessing the resistance of a microorganism, with population-
123 median resistance, heteroresistance and inoculum size impacting the resistance of a given inoculum,
124 nuances which are lost when an MIC at a single inoculum size is taken.

125

126 Materials and Methods

127 Yeast species and strains

128 Yeast species and strains used for experiments in this study are listed in Tables 1, 2 (alternative
129 identifiers and origin of isolation are given where available). Members of a large, initial
130 *Zygosaccharomyces* panel (Table S1) were designated *Z. bailii*, *Z. parabailii* or *Z. parabailii* based on
131 whole genome sequencing (WGS) analysis (see Genome sequencing) and a subset of these
132 comprised the main *Zygosaccharomyces* panel used for experiments (Table 1). Several species
133 previously designated *Z. bailii* were redesignated *Z. parabailii* or *Z. pseudobailii* based on the WGS
134 analysis (below). Members of a wide panel of isolates from more diverse yeast genera (Table S2)
135 were identified previously based on sequencing of the D1/D2 region of the 25S ribosomal DNA
136 (rDNA) (Stratford et al. 2013b).

137 Culture conditions

138 The YEPD growth medium used for culturing [20 g/l glucose, 20 g/l bacteriological peptone (Oxoid),
139 and 10 g/l yeast extract (Oxoid)] was adjusted to pH 4 using 5 M HCl prior to sterilisation by
140 autoclaving. Yeasts were stored at -80°C in cryovials in YEPD medium mixed with 0.2 volumes
141 glycerol. Cells were grown from frozen on YEPD supplemented with 2% agar (Oxoid) for 3 days at
142 30°C , before maintenance at 4°C for up to 3 weeks. For each biological replicate in experiments, a
143 single colony was suspended in 1 ml YEPD broth and, after determination of OD_{600} , an aliquot
144 transferred to 10 ml YEPD broth in order to give a starting $\text{OD}_{600}\sim 0.02$. These cultures were
145 incubated in 50 ml Erlenmeyer flasks at 24°C for >12 hours with shaking (120 rev/min) prior to use in
146 experiments at OD_{600} 0.1 – 2.0, when cells were growing in exponential phase. Desired
147 concentrations of sorbic acid in the growth medium were produced using a stock solution of 20 mM
148 potassium sorbate (Sigma-Aldrich) in YEPD, adjusted to pH 4 using 5 M HCl. Final concentrations of
149 sorbic acid in YEPD agar or broth were produced by mixing appropriate ratios of YEPD medium (pH

150 4) with the 20 mM sorbic acid-supplemented medium. All steps were carried out under aseptic
151 conditions.

152 De novo genome sequencing

153 *De novo* genome sequencing was carried out by KeyGene (Wageningen, Netherlands) by mapping
154 short Illumina reads to long PacBio reads for *Z. bailii* (7846), *Z. parabailii* (3699, containing *Z. bailii*-
155 derived 'A' genome and hybrid 'B' genome) and *Z. pseudobailii* (3697, containing *Z. bailii*-derived 'A'
156 genome and hybrid 'C' genome). Yeast isolates were grown in YEPD medium at 25°C for 48 hours.
157 Subsequently, cells were harvested by centrifugation (3000 *g*, 3 min), the supernatant removed and
158 the pelleted cultures freeze dried prior to DNA isolation. Isolation of high molecular weight DNA
159 suitable for long-read sequencing was carried out by Keygene based on methods described
160 previously (Zhang et al. 2012, Datema et al. 2016).

161 To generate the sequencing data for *Z. pseudobailii* and *Z. parabailii*, one PacBio SMRT cell (Sequel)
162 was used for each isolate. The same DNA was used for generating paired-end Illumina reads (MiSeq)
163 that was used for polishing of the PacBio data. To obtain the initial assembly of the two hybrid
164 species, *Z. parabailii* and *Z. pseudobailii*, the falcon-based HGAP 4 assembly method in SMRT Link
165 portal v7.0 from Pacific Biosciences was used. As the method already includes the error correction of
166 long reads, polishing was continued with Illumina short reads which has lower base calling error. The
167 assembly was polished three times using Pilon software version 1.22. The inverted full size contigs in
168 the assembly with respect to the reference genome were reverse complemented to make the
169 assembly compatible with public reference. The contigs which were partially inverted were left as
170 they were.

171 For the assembly of the *Z. bailii* genome, the sequencing library was prepared from PacBio high
172 fidelity (HiFi) reads, with lower error rate (similar to Illumina short reads), hence no polishing was
173 required. HiFi reads were obtained via circular consensus sequencing (CSS) from the SMRT Link
174 portal. The reads were then assembled into the draft assembly using the HiFi option of the Canu

175 assembler. The draft assembly was polished twice with HiFi reads using Racon software. Then, the
176 repetitive haplotypes were cleaned using the Purge Haplotigs pipeline. The remaining contigs were
177 checked for contamination by aligning the assembly to public reference, and by aligning a part of the
178 contigs to the BLASTn database. Finally, for all final assemblies of the three *Zygosaccharomyces*
179 subspecies, a BUSCO analysis was performed to check the completeness of genomes. The pairwise
180 alignments of genomes were done via the nucmer algorithm from the Mummer 4 package and
181 KeyGene's proprietary STL aligner (multi genome aligner). The multiple genome alignments (as pan
182 genomes) were visualized using Mauve software. All sequences used in this study were submitted to
183 the ENA under the study code PRJEB59101; *de novo* sequences were assigned the accession
184 numbers GCA_949129065, GCA_949129075 and GCA_949129085 for *Z. parabailii* (3699), *Z. bailii*
185 (7846) and *Z. pseudobailii* (3697), respectively.

186 Genome sequencing of the initial panel of *Zygosaccharomyces* isolates

187 The 111 isolates from the initial panel (Table S1) were cultured for 24 hours at 25°C in YEPD and
188 genomic DNA (gDNA) was isolated using the CTAB method (Stirling et al. 2003). Some gDNA samples
189 contained evidence of bacterial DNA, therefore, not all strains were included in the library
190 preparation and resequencing. Resequencing was performed by Illumina HiSeq4000 with 2x 125 bp,
191 on two lanes. For all Illumina sequencing, quality control was based on the QC30 threshold (80% of
192 reads with $\leq 0.1\%$ chance of miscalled base in all lanes of each run). The raw sequence data were
193 trimmed on a minimum base quality of 30 (Phred scores) and sequences with one or more N-
194 nucleotides were discarded. After trimming and filtering, read pairs for which both pairs had a
195 minimum read length of 50 nt were kept for further analysis. The pre-processed sequencing data
196 was mapped to the reference genome using BWA mem 0.7.17. Duplicated reads in the BAM file
197 were marked by Picard-tools MarkDuplicates (v1.63). SAMTOOLS (v1.3) was used to view, index, sort
198 and to merge the alignment files and the BAM files per sample genotyped using GATK 4. Variants
199 such as SNPs and INDELS were identified using GATK4 Haplotypecaller and were stored in a single

200 Variant Call Format (*.vcf) file. These variants were filtered on allele quality, sample quality and
201 allele depth. A minimum allele quality of 30, minimum sample quality of 20 and minimum allele
202 coverage depth of 7X were used for filtering. SNPs found in all samples that are identical were
203 discarded as they reflect errors in the reference sequence. The filtered variants were annotated
204 using the gene models with SNPeff. Most genes in *Z. parabailii* (3699) and *Z. pseudobailii* (3697)
205 were assigned to the A-subgenome (highly similar to the *Z. bailii* 7846 genome) or to the other
206 subgenome (i.e. B or C; see below). The long sequence aligner Blasr v1.3 was used in the
207 Bidirectional best hit approach to identify homologs. Only coding sequences were used for this
208 approach, extracted from the annotated gene models. Homologous genes with a high sequence
209 similarity (i.e. above 98%) to *Z. bailii* genes were assigned to the A-subgenome and genes below the
210 sequence similarity threshold were assigned to the B-subgenome (hybrid genome of *Z. parabailii*) or
211 C subgenome (hybrid genome of *Z. pseudobailii*). Phylogenetic trees were constructed based on
212 Genetic Distance Analysis of all open reading frames of sequences assigned to the A genome. The A
213 genome of each sequence was compared to the A genome of *Z. parabailii* reference strain 3699 and
214 an Unweighted pair group method with the given arithmetic mean (UPGMA) score (Khan et al.,
215 2008) assigned, from which a phylogenetic tree was constructed (Figure S5). All sequences used in
216 this study were submitted to the ENA under the study code PRJEB59101; strain-specific sample
217 numbers are quoted in Table S1.

218 Dose-response curve assay for heteroresistance

219 Yeasts were grown to exponential phase as described above and diluted in YEPD broth to OD₆₀₀
220 ~0.02 (inoculum size in 75 µl ~10,000 cells) or OD₆₀₀ 0.0002 (inoculum size in 75 µl ~100 cells). The
221 use of the different inocula allowed reliable determination of % viability across a wider range of
222 sorbic acid concentrations. Aliquots (75 µl) of each inoculum size were spread across 90 mm
223 diameter Petri dishes containing 20 ml YEPD agar supplemented with different concentrations of
224 sorbic acid (see above). After 21 days static incubation at 23°C, colony forming units (CFU) were

225 enumerated and percentage survival calculated by reference to control CFU counts on agar without
226 sorbic acid. At least three biological replicates were used in each experiment (exact numbers are
227 clarified in figure legends). Each of the biological replicates (from independent experiments) were
228 the average of three technical replicates for each sorbic acid concentration. Percentage survival data
229 was then fitted to a lognormal distribution curve in R software as detailed below (Fitting to normal
230 and lognormal distributions). Values derived with the curve fitting for IC_{50} , heteroresistance and
231 concentration at which 0.01% survival would be observed (MIC^{MODEL}) were recorded.

232 Inoculum-effect assay for heteroresistance

233 The inoculum effect (Steels et al. 2000) (Box 1) explains how experimentally measured MIC (MIC^{EXP})
234 can increase with size of the cell inoculum, as increased cell number increases the chance that the
235 inoculum includes phenotypically-variant cells that are hyper-resistant. Accordingly, the degree to
236 which the inoculum effect alters MIC^{EXP} is related to the extent of heteroresistance: MIC^{EXP} would
237 not be affected by inoculum size in a completely homogeneous cell population, whereas an impact
238 of increasing inoculum size on MIC^{EXP} will be greater the broader the range of single-cell resistances
239 (Figure 1A). It was reasoned that the magnitude of the inoculum effect could offer a novel,
240 convenient measure of heteroresistance. Dose-response curves of growth-inhibitory effect typically
241 follow a sigmoidal relationship (Stratford et al. 2013b) and have previously been modelled using Hill
242 functions, (Geoghegan et al. 2020, Stratford et al., 2019), indicating a normal frequency distribution
243 of single cell resistances. With that assumption, a relatively small number of MIC^{EXP} determinations
244 at defined inoculum sizes becomes sufficient for curve-fitting (Figure 1B, top panel), to enable
245 determination of standard deviation (σ) from the hypothetical normal distribution of cell resistances
246 (Figure 1B, bottom panel). This standard deviation reflects the extent of heteroresistance, as if the
247 difference between MIC^{EXP} values for different inoculum sizes increases, the normal distribution will
248 have a broader bell curve, reflecting increased heteroresistance. In addition, this curve can be

249 extrapolated to estimate the mean of the normal distribution, reflecting the population-median
250 resistance (IC_{50} , peak of the bell curve).

251 Pre-culture of yeasts was carried out as described above. Exponential phase cells were diluted to
252 $OD_{600} \sim 0.2$ (inoculum size in $75\mu\text{l} \sim 100,000$ cells) and serially diluted three times by 10-fold, giving a
253 lowest $OD_{600} \sim 0.0002$ (inoculum size in $75\mu\text{l} \sim 100$ cells). Aliquots ($75\mu\text{l}$) of each inoculum size were
254 transferred to wells of a flat-bottom, 96-well microplate (StarLab) and combined with $75\mu\text{l}$ of YEPD
255 broth pre-supplemented with sorbic acid at double the desired, final sorbic acid concentration. After
256 sealing with insulating tape, microplates were agitated at 600 rev/min for 60 s, placed in a sealed
257 plastic bag, and incubated statically at 23°C for 21 days. The presence or absence of growth was
258 noted visually under $\sim 2X$ magnification using a magnifying glass. The lowest concentration at which
259 no growth was detected in ≥ 1 of four technical replicates was scored as the experimental MIC
260 (MIC^{EXP}) for that inoculum from that biological replicate of the relevant isolate.

261 For inoculum effect measurements with the small panel of *Zygosaccharomyces* strains (Table S3),
262 the procedure was carried out as above but using inoculum sizes of 10^5 , 10^4 , 10^3 and 10^2 cells/well,
263 with concentration increments of 0.125 mM sorbic acid. For these particular assays, precise
264 inoculum size was verified by plating $75\mu\text{l}$ aliquots of the $OD_{600} \sim 0.0002$ suspension (100 cells) on
265 YEPD agar and incubating at 23°C for 7 days, the corresponding colony count was taken as the
266 inoculum size of the lowest inoculum. The MIC^{EXP} results were fitted to a normal or lognormal
267 distribution curve as described below.

268 Fitting to normal and lognormal distributions

269 Royston et al. (1982) describe a formula to determine the expected value of the maximum of n
270 random variables from a normal distribution (x_1, \dots, x_n), in terms of the theoretical mean (μ) and SD
271 (σ) of that distribution (Eq.1).

$$E[\max(x_1, \dots, x_n)] = \mu + \sigma * \text{qnorm}((n - \pi/8)/(n - \pi/4 + 1)) \quad (\text{Eq.1})$$

272

273 Assuming that the frequency distribution of antimicrobial resistance of n single cells from a
274 homogeneous cell culture is approximated by a normal (or log-normal) one, this equation can be
275 used to find the IC_{50} (the mean) and heteroresistance (the standard deviation) using data for MIC^{EXP}
276 and their corresponding inoculum sizes (x).

277 Equation 1 was fitted to experimental data using non-linear least squares fitting, by using the `nls()`
278 function in R, to return IC_{50} and heteroresistance values for each biological replicate. These were
279 then used to calculate MIC^{MODEL} by taking the concentration value at the 99.99th percentile of the
280 curve (where growth inhibition would occur in 99.99% of cells; Box 1). For each parameter, the mean
281 and standard error of the mean (SEM) across biological replicates were taken.

282 Plotting of curves for MIC^{EXP} versus inoculum size was carried out using the `ggplot` package in R.
283 Bootstraps to display 95% confidence interval of the line fitting were calculated using the `Boot`
284 function in the 'car' package in R.

285 For dose-response data, sorbic acid concentration values and their corresponding percentage
286 survival values were fitted to one minus a cumulative normal distribution function with mean and
287 standard deviation equal to the IC_{50} and heterogeneity, respectively. Fitting was done using
288 the `nls()` function in R software. Mean and SEM of each parameter were taken from the fitted curve
289 as for dose response curves detailed above.

290 Normal or lognormal distribution curves fitted to data were displayed in R (`ggplot` package), in the
291 case of inoculum effect data, and were displayed using the `plot()` function in MATLAB R20119b in the
292 case of dose-response curve data. Box and whisker plots, bar charts and correlation plots were
293 produced using Graphpad PRISM 9™ software. Correlations containing points with error bars were
294 produced using Microsoft Excel.

295 Simulations

296 Simulation of hypothetical normal distributions for single cell resistances of organisms (for
297 illustration of the inoculum effect concept) were produced using MATLAB R20119b. The Normal
298 Probability Density Function (normpdf) was used to plot frequency distributions for low and high
299 heteroresistance organisms ($\mu=5$, $\sigma=0.1$ and $\mu=5$, $\sigma=0.1$, respectively) with the frequency distribution
300 divided by ten to simulate the small inoculum size.

301 Data availability

302 All data are available in the present results section, in the supplemental material or on request.

303 Genome sequence accession or sample numbers (ENA) are given above and in Table S1.

304 Results

305 Use of the inoculum effect for determining heteroresistance

306 In order to assess the contributions made by phenotypic heterogeneity (specifically, sorbic acid
307 heteroresistance) and IC_{50} to the MIC, across large panels of species or strains, a new assay for
308 measuring these parameters was developed based on the ‘inoculum effect’ (See methods; Steels et
309 al. 2000), to allow higher throughput than traditional measurements of heteroresistance such as
310 from agar-based dose-response curve assays (Hewitt et al., 2016). Briefly, this method fitted a
311 normal distribution curve of single cell resistances to experimental MIC (MIC^{EXP}) values, by modelling
312 MIC^{EXP} for a given inoculum as its corresponding point on the normal distribution curve (Figure 1B,
313 top), e.g., MIC^{EXP} for 100 cells/well is the point where 1 in 100 cells would survive, MIC^{EXP} for 1000
314 cells/well is the point where 1 in 1000 cells would survive, etc. (see Methods). The median and
315 standard deviation of the fitted normal distribution curve (Figure 1B, bottom) could then be taken as
316 the IC_{50} and heteroresistance respectively.

317 For purposes of curve fitting, lognormal distributions were adopted as these gave better fit to dose
318 response curve data than normal distributions (Figure S1). In addition, possible effect specifically of
319 cell density (cell concentration) on the probability of growth occurring in a well was evaluated, e.g.,
320 due to stressor saturation or quorum sensing-type phenomena, as such effect could complicate
321 interpretation of the inoculum effect which infers a total cell number effect. Only a minor possible
322 effect of cell density was apparent, and similarly in high or low heteroresistance isolates (Figure S2).
323 This result supported the inference that differences measured with inoculum effect methodology
324 primarily reflected differences in heteroresistance rather than effects attributable to altered cell
325 density.

326 To further assess the use of the inoculum effect method, IC_{50} (Figure 2A), heteroresistance (Figure
327 2B) and MIC (Figure 2C) determinations for six randomly selected strains from the

328 *Zygosaccharomyces* panel (Table 1) were compared between the inoculum effect method and the
329 dose-response curve method. The parameter MIC^{MODEL} was also taken, defined as the lowest
330 concentration giving 99.99% inhibition of cell growth (Box 1) and consistent with previous
331 publications in this field (Stratford et al. 2013b, 2014). This was calculated using the equation for the
332 lognormal distribution curve fitted to MIC^{EXP} data (as in Figure 1B). For inoculum effect assays
333 (carried out in broth), heteroresistance showed a moderately strong, significant correlation with
334 heteroresistance values derived from dose-response curves ($r=0.74$), while IC_{50} and MIC^{MODEL} also
335 showed strong correlations between the assays ($r=0.853$ and 0.865 , respectively). The inoculum
336 effect assay was repeated on agar to assess possible effects of broth- versus agar-based assay
337 formats (as in the above comparison) on the outcomes (Figure S3). Similar correlations were
338 obtained as above indicating that for all the test parameters (IC_{50} , heteroresistance and MIC^{MODEL}),
339 dose response results generally compare well with inoculum effect results obtained either in broth
340 or on agar. These results supported use of the inoculum effect methodology, using a lognormal
341 distribution for data, as an alternative heteroresistance assay to the established, but time-
342 consuming dose-response curve method. Further assays below used the broth condition for
343 inoculum effect assay, which offers higher throughput than on agar and is a condition also more
344 relevant to the beverages and other product types in which sorbic acid is normally used.

345 High-throughput determination of survival parameters for *Zygosaccharomyces* isolates

346 To investigate relationships between heteroresistance or IC_{50} with MIC^{MODEL} , we applied the
347 inoculum effect methodology to a panel of *Zygosaccharomyces* sp. Isolates. To select strains for
348 study, an initial panel of 111 yeasts isolated from foods (see Table S1) were whole-genome
349 sequenced (WGS); most of these had previously been considered as *Z. bailii* isolates (Stratford et al.
350 2013b, 2014, 2019). The sequencing revealed that several isolates previously characterised as *Z.*
351 *bailii* were in fact *Z. parabailii* or *Z. pseudobailii* (see Methods). These species are known interspecies
352 hybrids formed between *Z. bailii* and unknown, closely related ancestors. From these 111 isolates,

353 for further study a panel of 29 strains were selected, to include isolates sampled from across the
354 span of the phylogenetic tree (Figure S5) and diverse sources of isolation. This ‘Main
355 *Zygosaccharomyces* panel’ comprised 5, 17 and 7 isolates of *Z. bailii*, *Z. parabailii* and *Z. pseudobailii*
356 respectively (Table 1). For parameter measurement (heteroresistance, IC_{50} and MIC^{MODEL}) inoculum
357 effect methodology was used, with curves fitted to MIC^{EXP} values taken at 10^5 and 10^2 cells/well.
358 There was considerable variation in heteroresistance, IC_{50} , and MIC^{MODEL} among isolates of the panel,
359 with ranges of approximately 0.03–0.11, 2.3–5.4 and 4.3–9.2 mM for heteroresistance, IC_{50} and
360 MIC^{MODEL} , respectively (Table 1; Figure 3A). Analysis for each subspecies indicated that *Z. pseudobailii*
361 had a significantly greater mean heteroresistance than *Z. parabailii* and *Z. bailii*, whereas the mean
362 IC_{50} for *Z. pseudobailii* was significantly lower than for *Z. parabailii* (Figure 3B). There were no
363 significant differences in average MIC^{MODEL} between the different subspecies (two sample t-test
364 assuming unequal variances), although there was both a broader spread of values and relatively low
365 mean for *Z. bailii* isolates (Figure 3B).

366 To further investigate the relationships between heteroresistance, IC_{50} and MIC^{MODEL} , the correlation
367 between these parameters was calculated. Across the main *Zygosaccharomyces* panel of 29 strains,
368 strains with high IC_{50} tended to have high MIC^{MODEL} and *vice versa* ($r=0.675$, $p<0.0001$), whereas
369 heteroresistance was not significantly correlated with MIC^{MODEL} ($r=0.326$, $p=0.08$) (Figure 4A).
370 Unexpectedly, strains with a high IC_{50} tended to have a low heteroresistance ($r=0.586$, $p<0.01$)
371 (Figure 4A). When the subspecies were examined independently, *Z. bailii* (Figure 4B), *Z. parabailii*
372 (Figure 4C) and *Z. pseudobailii* (Figure 4D) also each showed a significant correlation between IC_{50} and
373 MIC^{MODEL} and no significant correlation between heteroresistance and MIC^{MODEL} . In the case of *Z.*
374 *parabailii*, it was noted that calculated correlations were strongly influenced by a single isolate
375 (3698) with a much lower IC_{50} than all the other *Z. parabailii* isolates (Figure 4C). When the *Z.*
376 *parabailii* dataset was analysed without this single isolate ($n=16$), heteroresistance was strongly
377 correlated with MIC^{MODEL} ($r=0.660$, $p<0.01$) and IC_{50} was not ($r=0.265$, $p=0.32$) (Figure S4). The
378 correlation between heteroresistance and MIC^{MODEL} in this sample could suggest that

379 heteroresistance is more strongly related to MIC^{MODEL} when variation in IC_{50} is relatively limited, as
380 was the case in *Z. parabailii* after removal of isolate 3698 (see Discussion).

381 Trends in heteroresistance, IC_{50} and MIC^{MODEL} across a wide panel of diverse yeast species

382 To investigate if the trends in sorbic acid heteroresistance described above may be replicated in
383 other spoilage yeast species, dose response curve data from a 'wide panel' of spoilage yeasts isolates
384 (Table S2) produced in a previous survey were analysed. These isolates encompassed 26 species
385 from 12 different yeast genera. Three *Z. parabailii* and two *S. cerevisiae* strains were present in the
386 panel, whereas all other species were represented by one isolate only. To avoid mixing intra- with
387 inter-species comparisons, values averaged across the three *Z. parabailii* and across the two *S.*
388 *cerevisiae* isolates were used for these two species. This wide yeast panel produced a notably wider
389 range of IC_{50} and MIC^{MODEL} values than the main *Zygosaccharomyces* panel (Figure 5A,B). This was
390 primarily due to comparatively low IC_{50} and MIC^{MODEL} values for certain species of the wide panel,
391 such as *Rhodotorula mucilaginosa* (IC_{50} ~0.337mM, MIC^{MODEL} ~0.467 mM) and *Zygosaccharomyces*
392 *rouxii* (IC_{50} ~1.34mM, MIC^{MODEL} ~2.45mM), two species previously associated with food environments
393 where sorbic acid is not used (Pitt & Hocking, 2009). The two panels exhibited similar variation in
394 heteroresistance between isolates, but the *Zygosaccharomyces* isolates showed significantly higher
395 mean heteroresistance ($p < 0.0001$) (Figure 5B). IC_{50} was very strongly correlated with MIC^{MODEL} in the
396 wide panel ($r=0.986$, $p < 0.0001$) (Figure 5C). The wide panel also showed a weaker correlation
397 between heteroresistance and MIC^{MODEL} ($r = 0.487$, $p < 0.05$). There was a weak, non-significant
398 correlation between heteroresistance and IC_{50} , which was weaker than that with MIC^{MODEL}
399 suggesting that the relationship between heteroresistance and MIC^{MODEL} was not simply a reflection
400 of the strong relationship between IC_{50} and MIC^{MODEL} . The results collectively indicate a close
401 relationship between MIC and population-median resistance (IC_{50}) and additionally, albeit relatively
402 weakly, with heteroresistance, as discussed below.

403

405 Discussion

406 This study showcases the relevance of IC_{50} and heteroresistance parameters for an inhibitor's MIC
407 against organisms, here focussing on the preservative sorbic acid. The novel, high-throughput
408 inoculum effect methodology developed here allowed heteroresistance to be determined in a large
409 number of microorganisms, in a manner less laborious than an established method like dose-
410 response assay on agar. In addition, the microplate format of the new assay demands only modest
411 physical incubator space and is amenable to automation. This methodology offers the potential for
412 screens of heteroresistance in new ecological or industrial contexts, for example in modelling and
413 quantitative risk assessments in the food industry. Our results indicate that a dominant indicator of
414 differences in MIC between strains is differences in IC_{50} , with heteroresistance (e.g. incidence of
415 rare, hyper-resistant cells) playing a smaller role.

416 The experimental data were consistent with lognormal distributions of single-cell resistances in the
417 yeast cell populations. Hill functions have previously been employed to model dose response curves
418 using \log_{10} values for stressor concentration (Geoghegan et al., 2020; Stratford et al. 2019), a model
419 which assumes single-cell resistances are lognormally distributed. Here, while the fit of the
420 lognormal distribution curve to the data was only marginally better than a normal distribution, for
421 this study we were more interested in differences in relative distributions of single cell resistances,
422 therefore lognormal was suited to the study's aims.

423 The possibility that cell-concentration may make a contribution to the inoculum effect that is
424 independent of effects due to resistant-cell incidence was investigated, e.g., arising from stressor
425 saturation or quorum sensing-type phenomena, for example. Some previous reports of the inoculum
426 effect have not made this distinction (Loffredo et al. 2020, Smith et al., 2018). However, Scheler et
427 al. (2020) demonstrated that inoculum effect in *E. coli* for cefotaxime resulted from heteroresistance
428 rather than cell concentration, while Steels et al. (2000) ruled out certain effects of cell
429 concentration (e.g. altered adsorption) in the inoculum effect of *Z. bailii* with sorbic acid. On the

430 other hand, cell concentration affected survival probability of heat-shocked *S. cerevisiae*, attributed
431 to cooperative glutathione excretion at high cell density (Laman Trip & Youk, 2020). To our
432 knowledge, no such mechanisms have been reported for sorbic acid stress. Here, analyses indicated
433 that cell concentration may make only a minor contribution to the increasing sorbic acid MIC^{MODEL} as
434 inoculum size was increased (between 10² and 10⁴ cells per well). One possible explanation for that
435 small effect could be related to the documented metabolism of sorbic acid by *Z. bailii* (Mollapour
436 and Piper, 2001).

437 Heteroresistance, IC₅₀ and MIC^{MODEL} values obtained on agar (from dose response assay) showed
438 significant correlation with the same parameters obtained in broth (from inoculum effect assay).
439 This consistency for all three parameters whether measured in broth or agar is in line with work
440 elsewhere reporting similar resistances to other stressors in broth versus agar (Morris et al., 2020;
441 Albano et al., 2021; Fuchs et al., 2021). Robustness of the heteroresistance phenotype to the form of
442 growth environment is consistent with heteroresistance being an intrinsic property of cell
443 populations, not strongly affected by environment. This property allows resistant subpopulations to
444 arise independent of stressor exposure, for example, so enabling pre-priming for possible future
445 perturbations. Such pre-priming of heteroresistance has been described for other stressor scenarios
446 (Jing et al. 2018, Levy et al., 2012; Stratford et al. 2014), and is in line with understanding of the
447 wider premise for phenotypic heterogeneity, or bet-hedging (Avery, 2006; Ackermann, 2015).

448 There was considerable variation in all three parameters between strains and species of the
449 *Zygosaccharomyces* genus and across a wider panel of spoilage yeast species. *Z. bailii* is considered
450 as more heteroresistant to sorbic acid than *S. cerevisiae* (Stratford et al. 2014). Across the main
451 *Zygosaccharomyces* panel and the constituent subspecies, IC₅₀ was more clearly correlated with
452 MIC^{MODEL} than was heteroresistance. However, in the case of *Z. parabailii* this trend was reversed by
453 the removal of a single outlying strain with an uncharacteristically low IC₅₀ value. The removal of this
454 outlier considerably reduced the variation in IC₅₀ for the subspecies (standard deviation reduced to

455 0.055 from 0.076) but had negligible impact on variation in heteroresistance (standard deviations
456 0.0188 and 0.0186). This could suggest that relationships between heteroresistance and MIC are
457 masked when IC_{50} variation is high and potentially dominating effects on MIC across different
458 organisms. Accordingly, heteroresistance may be more important for MIC in species or contexts that
459 support lower variation in IC_{50} .

460 Regarding the question of why one (sub-)species might evolve a higher average preservative
461 heteroresistance than others (e.g. *Z. pseudobailii*, Figure 3B), drivers could be related to the
462 organisms' ecologies or relative incidences. This may include the size of inoculum typically
463 associated with spoilage incidence of an organism, as larger inocula could amplify the effect that
464 heteroresistance has on the MIC. Alternatively, the frequency of transition of the growth
465 environment from preservative-rich to -poor, as frequent changes are thought to favour high
466 heterogeneity (Avery, 2006). Modelling of gene expression patterns has indicated that gene
467 expression noise confers a stronger fitness advantage when population-averaged gene expression is
468 further from the optimal level (Duveau et al. 2018), a situation more often encountered in
469 fluctuating environments. Regarding the particular example of this study, a less stable niche for *Z.*
470 *pseudobailii* is partially supported by this organism being found primarily in viscous foodstuffs (Table
471 1), although a similar argument could be made for *Z. parabailii* (where average heteroresistance was
472 lower) which colonises solid as well as liquid foodstuffs.

473 There was a negative correlation between heteroresistance and IC_{50} across the main
474 *Zygosaccharomyces* panel. One suggestion to explain this might be that heteroresistance is more
475 strongly selected in low- IC_{50} strains in compensation for a disparity between their population-
476 median resistance (IC_{50}) and optimal resistance when faced with stressor. That would be in line with
477 other previously described scenarios, including the example mentioned above where noisy gene
478 expression is especially beneficial when average gene expression is far from the optimum (Duveau et
479 al. 2018).

480 Other trends were evident here across a wider panel of spoilage yeast species. In particular, a weak
481 but significant positive correlation between heteroresistance and MIC emerged. This suggests that
482 heteroresistance may make a larger contribution to MIC differences between distantly related
483 species of spoilage yeasts than across individual isolates of the *Zygosaccharomyces* genus. At the
484 same time, a correlation between IC₅₀ and MIC in the wide panel was stronger than in the main
485 *Zygosaccharomyces* panel, possibly reflecting the wider range of IC₅₀ phenotypes across the wide
486 panel. While specific trends were different between the two panels the overall conclusion was
487 similar, that IC₅₀ is more closely related than heteroresistance to preservative MIC.

488 Why heteroresistance has not been strongly associated with sorbic acid resistance in this study
489 requires consideration. One explanation is that if the metabolic cost to a cell of resisting sorbic acid
490 stress is low, the fitness benefit of bet-hedging over increasing population-average resistance would
491 be reduced. While some strategies for sorbic acid resistance such as increased expression of efflux
492 pumps (Geoghegan et al. 2020) would be metabolically costly, favouring heteroresistance (Jing et al.
493 2018), other proposed resistance mechanisms such as potential maintenance of a more
494 fermentative metabolism (Stratford et al. 2020) might confer resistance at a comparably low cost,
495 mitigating the fitness benefit of heteroresistance over IC₅₀. It is possible that stronger
496 heteroresistance phenotypes would be found in niches where the metabolic cost of pre-priming (all)
497 cells for stress was greater. A possibly-related observation was overrepresentation of the high-IC₅₀,
498 low-heteroresistance species *Z. parabailii* in the initial *Zygosaccharomyces* panel used in this study
499 (n=71, 19 and 21 for *Z. parabailii*, *Z. pseudobailii* and *Z. bailii* respectively, Table S1). As this reflects
500 isolation of *Z. parabailii* from a larger number of food spoilage events, it is consistent with the
501 suggestion that a high IC₅₀ as opposed to high heteroresistance may be a more effective evolutionary
502 strategy for growing in preserved foods, though of course we cannot discount that other traits of *Z.*
503 *parabailii* account for its preponderance. It should also be noted that this study was limited to food
504 spoilage isolates only and other relationships may be manifest in other ecological niches.

505 Conclusion

506 We capitalised on the inoculum effect principle to develop a new, high-throughput method for
507 assaying heteroresistance. Application of this assay to diverse spoilage yeasts revealed that
508 heteroresistance and especially IC₅₀ are related to MIC, whereas a relationship with heteroresistance
509 was not observed when considering a panel only of *Zygosaccharomyces* sp. isolates. Overall, IC₅₀
510 appears to be a strong indicator of MIC, but heteroresistance may also be related to MIC between
511 distantly related species or in contexts where IC₅₀ variation is low. This work highlights certain
512 limitations of conventional MIC measurements as, due to the effect of heteroresistance, the
513 apparent resistance of an organism could vary markedly according to inoculum size. The average
514 resistance of a cell population, its heteroresistance and the inoculum size should all be considered in
515 selecting appropriate antimicrobial concentrations for specific applications, e.g., food preservation.
516 In experimental work (e.g. in microbial challenge testing) this would translate to using an adequate
517 population size (e.g. 10⁴ cells) in the desired test volume.

518

519 Acknowledgements

520 This work was supported by the Biotechnology and Biological Sciences Research Council (grant
521 number B/T508949/1). We thank Malcolm Stratford for kindly sharing yeast isolates and data.

522

523 References

- 524 ACKERMANN, M. 2015. A functional perspective on phenotypic heterogeneity in microorganisms.
525 Nature Reviews Microbiology, 13, 497-508.
- 526 ALBANO, M., KARAU, M. J., SCHUETZ, A. N. & PATEL, R. 2020. Comparison of agar dilution to broth
527 microdilution for testing in vitro activity of cefiderocol against Gram-negative bacilli. Journal of
528 Clinical Microbiology, 59, e00966-20.
- 529 ANDERSSON, D. I., NICOLOFF, H. & HJORT, K. 2019. Mechanisms and clinical relevance of bacterial
530 heteroresistance. Nature Reviews Microbiology, 17, 479-496.
- 531 BISHOP, A. L., RAB, F. A., SUMNER, E. R. & AVERY, S. V. 2007. Phenotypic heterogeneity can enhance
532 rare-cell survival in 'stress-sensitive' yeast populations. Molecular Microbiology, 63, 507-520.
- 533 BRAUN-GALLEANI, S., ORTIZ-MERINO, R. A., WU, Q., XU, Y. & WOLFE, K. H. 2018. *Zygosaccharomyces*
534 *pseudobailii*, another yeast interspecies hybrid that regained fertility by damaging one of its *MAT*
535 loci. FEMS Yeast Research, 18, foy079.
- 536 DATEMA, E., HULZINK, R. J., BLOMMERS, L., VALLE-INCLAN, J. E., VAN ORSOUW, N., WITTENBERG, A.
537 H. & DE VOS, M. 2016. The megabase-sized fungal genome of *Rhizoctonia solani* assembled from
538 nanopore reads only. bioRxiv, 084772.
- 539 DAVIES, C. R., WOHLGEMUTH, F., YOUNG, T., VIOLET, J., DICKINSON, M., SANDERS, J.-W., VALLIERES,
540 C. & AVERY, S. V. 2021. Evolving challenges and strategies for fungal control in the food supply chain.
541 Fungal Biology Reviews, 36, 15-26.
- 542 DEWACHTER, L., FAUVART, M. & MICHIELS, J. 2019. Bacterial heterogeneity and antibiotic survival:
543 understanding and combatting persistence and heteroresistance. Molecular Cell, 76, 255-267.

- 544 DUVEAU, F., HODGINS-DAVIS, A., METZGER, B. P., YANG, B., TRYBAN, S., WALKER, E. A., LYBROOK, T.
545 & WITTKOPP, P. J. 2018. Fitness effects of altering gene expression noise in *Saccharomyces*
546 *cerevisiae*. eLife, 7, e37272.
- 547 FUCHS, F., HOF, H., HOFMANN, S., KURZAI, O., MEIS, J. F. & HAMPRECHT, A. 2021. Antifungal activity
548 of nitroxoline against *Candida auris* isolates. Clinical Microbiology and Infection, 27, 1697.e7-
549 1697.e10.
- 550 GEOGHEGAN, I. A., STRATFORD, M., BROMLEY, M., ARCHER, D. B. & AVERY, S. V. 2020. Weak acid
551 resistance A (WarA), a novel transcription factor required for regulation of weak-acid resistance and
552 spore-spore heterogeneity in *Aspergillus niger*. mSphere, 5, e00685-19.
- 553 HEWITT, S. K., FOSTER, D. S., DYER, P. S. & AVERY, S. V. 2016. Phenotypic heterogeneity in fungi:
554 importance and methodology. Fungal Biology Reviews, 30, 176-184.
- 555 HOLLAND, S. L., READER, T., DYER, P. S. & AVERY, S. V. 2014. Phenotypic heterogeneity is a selected
556 trait in natural yeast populations subject to environmental stress. Environmental Microbiology, 16,
557 1729-1740.
- 558 JING, W., CAMELLATO, B., RONEY, I. J., KAERN, M. & GODIN, M. 2018. Measuring single-cell
559 phenotypic growth heterogeneity using a microfluidic cell volume sensor. Scientific Reports, 8, 1-10.
- 560 KHAN, H. A., ARIF, I. A., BAHKALI, A. H., FARHAN, A. H. A. & HOMAIDAN, A. A. A. 2008. Bayesian,
561 maximum parsimony and UPGMA models for inferring the phylogenies of antelopes using
562 mitochondrial markers. Evolutionary Bioinformatics, 4, EBO.S934.
- 563 LAMAN TRIP, D. S. & YOUK, H. 2020. Yeasts collectively extend the limits of habitable temperatures
564 by secreting glutathione. Nature Microbiology, 5, 943-954.
- 565 LEVY, S. F., ZIV, N. & SIEGAL, M. L. 2012. Bet hedging in yeast by heterogeneous, age-correlated
566 expression of a stress protectant. PLoS Biology, 10, e1001325.

- 567 LINDAHL, L., GENHEDEN, S., ERIKSSON, L. A., OLSSON, L. & BETTIGA, M. 2016. Sphingolipids
568 contribute to acetic acid resistance in *Zygosaccharomyces bailii*. Biotechnology and Bioengineering,
569 113, 744-753.
- 570 LINDBERG, L., SANTOS, A. X., RIEZMAN, H., OLSSON, L. & BETTIGA, M. 2013. Lipidomic profiling of
571 *Saccharomyces cerevisiae* and *Zygosaccharomyces bailii* reveals critical changes in lipid composition
572 in response to acetic acid stress. PloS One, 8, e73936.
- 573 LIU, J., LESTRADE, D., ARABACIYAN, S., CESCUT, J., FRANÇOIS, J.-M. & CAPP, J.-P. 2018. A *GRX1*
574 promoter variant confers constitutive noisy bimodal expression that increases oxidative stress
575 resistance in yeast. Frontiers in Microbiology, 9, 2158.
- 576 LOFFREDO, M. R., SAVINI, F., BOBONE, S., CASCIARO, B., FRANZYK, H., MANGONI, M. L. & STELLA, L.
577 2021. Inoculum effect of antimicrobial peptides. Proceedings of the National Academy of Sciences,
578 118, e2014364118.
- 579 MOLLAPOUR, M. & PIPER, P. W. 2001. The *ZbYME2* gene from the food spoilage yeast
580 *Zygosaccharomyces bailii* confers not only *YME2* functions in *Saccharomyces cerevisiae*, but also the
581 capacity for catabolism of sorbate and benzoate, two major weak organic acid preservatives.
582 Molecular Microbiology, 42, 919-930.
- 583 MORRIS, C. P., BERGMAN, Y., TEKLE, T., FISSEL, J. A., TAMMA, P. D. & SIMNER, P. J. 2020. Cefiderocol
584 antimicrobial susceptibility testing against multidrug-resistant Gram-negative bacilli: a comparison of
585 disk diffusion to broth microdilution. Journal of Clinical Microbiology, 59, e01649-20.
- 586 NEWMAN, J. R., GHAEMMAGHAMI, S., IHMELS, J., BRESLOW, D. K., NOBLE, M., DERISI, J. L. &
587 WEISSMAN, J. S. 2006. Single-cell proteomic analysis of *S. cerevisiae* reveals the architecture of
588 biological noise. Nature, 441, 840-846.
- 589 PITT, J. I. & HOCKING, A. D. 2009. Fungi and food spoilage, 3rd ed. Springer, New York.
- 590 ROYSTON, J. P. 1982. Journal of the Royal Statistical Society. Series C (Applied Statistics), 31, 161-165

591 SCHELER, O., MAKUCH, K., DEBSKI, P. R., HORKA, M., RUSZCZAK, A., PACOCHA, N., SOZAŃSKI, K.,
592 SMOLANDER, O.-P., POSTEK, W. & GARSTECKI, P. 2020. Droplet-based digital antibiotic susceptibility
593 screen reveals single-cell clonal heteroresistance in an isogenic bacterial population. Scientific
594 Reports, 10, 1-8.

595 SILANDER, O. K., NIKOLIC, N., ZASLAVER, A., BREN, A., KIKOIN, I., ALON, U. & ACKERMANN, M. 2012.
596 A genome-wide analysis of promoter-mediated phenotypic noise in *Escherichia coli*. PLoS genetics, 8,
597 e1002443.

598 SMITH, K. P. & KIRBY, J. E. 2018. The inoculum effect in the era of multidrug resistance: minor
599 differences in inoculum have dramatic effect on MIC determination. Antimicrobial Agents and
600 Chemotherapy, 62, e00433-18.

601 SMITH, M. C., SUMNER, E. R. & AVERY, S. V. 2007. Glutathione and Gts1p drive beneficial variability
602 in the cadmium resistances of individual yeast cells. Molecular Microbiology, 66, 699-712.

603 STEELS, H., JAMES, S.A., ROBERTS, I.N. & STRATFORD M. 2000. Sorbic acid resistance: the inoculum
604 effect. Yeast, 16, 1173-1183

605 STIRLING, D. 2003. DNA extraction from fungi, yeast, and bacteria. In Methods in Molecular Biology:
606 PCR Protocols, Vol. 226, 2nd ed., ed. by Bartlett, J. M. S. & Stirling, D., Humana Press Inc., Totowa,
607 NJ, U.S.A., pp. 53–54.

608 STRATFORD, M., NEBE-VON-CARON, G., STEELS, H., NOVODVORSKA, M., UECKERT, J. & ARCHER, D.
609 B. 2013. Weak-acid preservatives: pH and proton movements in the yeast *Saccharomyces cerevisiae*.
610 International journal of food microbiology, 161, 164-171.

611 STRATFORD, M., STEELS, H., NEBE-VON-CARON, G., AVERY, S. V., NOVODVORSKA, M. & ARCHER, D.
612 B. 2014. Population heterogeneity and dynamics in starter culture and lag phase adaptation of the
613 spoilage yeast *Zygosaccharomyces bailii* to weak acid preservatives. International journal of food
614 microbiology, 181, 40-47.

615 STRATFORD, M., STEELS, H., NEBE-VON-CARON, G., NOVODVORSKA, M., HAYER, K. & ARCHER, D. B.
616 2013. Extreme resistance to weak-acid preservatives in the spoilage yeast *Zygosaccharomyces bailii*.
617 International Journal of Food Microbiology, 166, 126-134.

618 STRATFORD, M., STEELS, H., NOVODVORSKA, M., ARCHER, D. B. & AVERY, S. V. 2019. Extreme
619 osmotolerance and halotolerance in food-relevant yeasts and the role of glycerol-dependent cell
620 individuality. Frontiers in Microbiology, 9, 3238.

621 STRATFORD, M., VALLIÈRES, C., GEOGHEGAN, I. A., ARCHER, D. B. & AVERY, S. V. 2020. The
622 preservative sorbic acid targets respiration, explaining the resistance of fermentative spoilage yeast
623 species. mSphere, 5, e00273-20.

624 URCHUEGUÍA, A., GALBUSERA, L., CHAUVIN, D., BELLEMENT, G., JULOU, T. & VAN NIMWEGEN, E.
625 2021. Genome-wide gene expression noise in *Escherichia coli* is condition-dependent and
626 determined by propagation of noise through the regulatory network. PLoS Biology, 19, e3001491.

627 ZHANG, M., ZHANG, Y., SCHEURING, C. F., WU, C.-C., DONG, J. J. & ZHANG, H.-B. 2012. Preparation
628 of megabase-sized DNA from a variety of organisms using the nuclei method for advanced genomics
629 research. Nature Protocols, 7, 467-478.

630

631

632

633 **Table 1: Main panel of *Zygosaccharomyces* strains, including sorbic acid resistance values.**

Strain	Alternative reference	Species*	Isolation Source/location	Heteroresistance (SD, mM)	IC ₅₀ (mM)	MIC ^{MODEL} (mM)
1730		<i>Z. pseudobailii</i>	Ketchup	0.0648 ^a	3.77	6.69
3697		<i>Z. pseudobailii</i>	low fat tartare sauce	0.0899	3.16	7.00
3698		<i>Z. parabailii</i>	Chow chow	0.0726	2.41	4.57
3699		<i>Z. parabailii</i>	Creamy caesar dressing	0.0453	3.59	5.36
3704		<i>Z. parabailii</i>	Ketchup, Russia, 2003	0.0436	4.40	6.47
3942		<i>Z. parabailii</i>	Yoghurt mayonnaise	0.0828	3.40	7.07
3959		<i>Z. parabailii</i>	Ice Tea concentrate	0.1054	3.56	9.04
7406		<i>Z. parabailii</i>	Peach ice tea production environment, Nigeria	0.0688	4.06	7.46
7445		<i>Z. parabailii</i>	Ice tea, Mexico	0.0689	3.58	6.58
7768		<i>Z. bailii</i>	Spoiled Ice Tea concentrate, Portugal	0.0673	5.06	9.18
7769		<i>Z. pseudobailii</i>	Tartare Sauce, Poland, 2019	0.0760	3.63	7.11
7777	DBVPG 6378, CECT11933	<i>Z. parabailii</i>	Mayonnaise, Netherlands	0.0456	4.08	6.11
7788	CBS 6708	<i>Z. bailii</i>	Orange-juice concentrate, Brazil	0.0502	4.11	6.40
7800	MUCL 38950	<i>Z. bailii</i>	fermented tea, 1994	0.0635	2.71	4.76
7807	MUCL 55123	<i>Z. parabailii</i>	Alcoholic fermented beverage, 2012	0.0538	3.76	6.05
7809	2, CBS 685, NCYC 563	<i>Z. pseudobailii</i>	UK	0.0857	2.32	4.95
7812	6 ^{b,c,d}	<i>Z. parabailii</i>	Bottled ice tea, USA	0.0458	4.09	6.13
7820	15 ^{b,c,d}	<i>Z. pseudobailii</i>	Salad dressing, Netherlands	0.0719	3.05	5.77
7829	105 ^{b,c,d} , NCYC 2933,	<i>Z. parabailii</i>	Tomato based product, UK, 2000	0.0897	3.37	7.46
7836	194 ^{b,c,d} DBVPG 6924	<i>Z. pseudobailii</i>	Honey, China	0.0643	3.28	5.80

7838	362 ^{b,c,d}	<i>Z. parabailii</i>	Factory isolate, Turkey	0.0345	4.35	5.91
7842	592 ^{b,c,d} NCYC 3378	<i>Z. parabailii</i>	Soft Drinks factory, Phillipines, 2006	0.0520	4.93	7.82
7843	593 ^{b,c,d} NCYC 3379	<i>Z. bailii</i>	Factory isolate, Phillipines, 2006	0.0653	2.92	5.20
7851	NCYC 464	<i>Z. pseudobailii</i>	Sweet pickle, 1955	0.0935	3.01	6.88
7852	NCYC 573	<i>Z. bailii</i>	Red wine, USA, 1959	0.0380	3.06	4.28
7862	NRRL Y-11865	<i>Z. parabailii</i>	Salad Cream, 1985	0.0537	3.79	6.09
7870		<i>Z. parabailii</i>	Unknown source, Belgium	0.0453	5.38	8.03
7871		<i>Z. parabailii</i>	Ice Tea concentrate, Guatemala, 2019	0.0647	4.22	7.49
7873		<i>Z. parabailii</i>	Yoghurt, Czech Republic, 2019	0.0637	3.52	6.19

634 * verified by WGS analysis (see below)

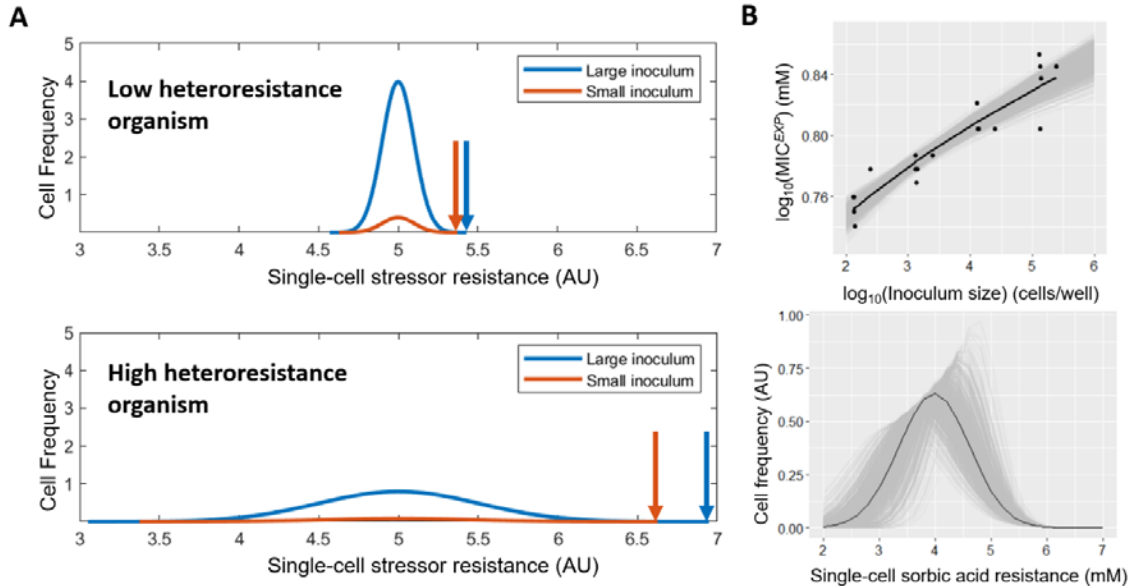
635 ^a error values for heteroresistance, IC⁵⁰ and MIC^{MODEL} are shown in Figure 3a

636 ^b as designated by Stratford et al 2019

637 ^c as designated by Stratford et al. 2020

638 ^d as designated by Stratford et al 2013b

639

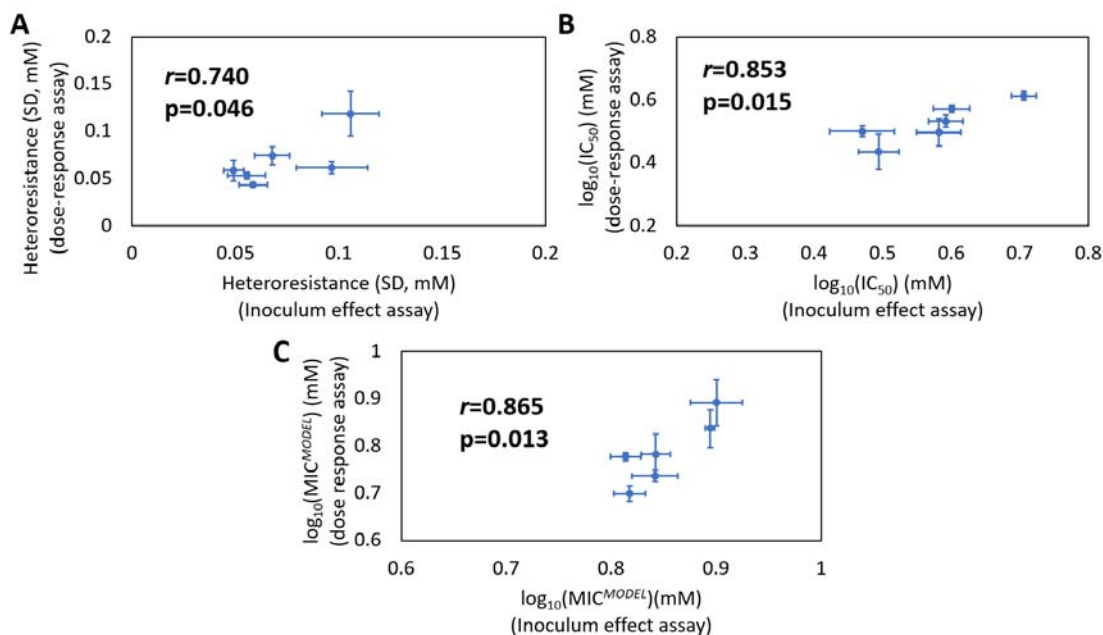


640

641

642 **Figure 1: Establishing parameters for quantifying heteroresistance via the inoculum effect. (A)** Modelled
643 single-cell frequency distributions of stressor resistance (hypothetical) in low- and high-heteroresistance cell
644 populations, at large and small inoculum sizes; these are modelled assuming single-cell resistances are
645 normally distributed in the populations, with the total area under each curve equalling 1 and 0.1 for large and
646 small inocula, respectively. Plots intersect the x-axis where survivor-cell frequency decreases below 0.001,
647 corresponding to the theoretical point at which less than one cell of the relevant inoculum survives and
648 equating to the MIC, indicated with an arrow. AU, arbitrary units. **(B)** Top panel: normal distribution curve
649 fitted to MIC^{EXP} (Box 1) values for sorbic acid resistance (mM) at four optical densities (each with six replicates
650 normalised to cells/well according to corresponding colony counts on agar) using inoculum effect methodology
651 (see Methods) for strain 7812 (n=6 biological replicates). Black line, line of best fit. Grey lines, simulated
652 normal distributions, with the distance between the upper and lower lines for each x value representing the
653 95% confidence interval for that point. Bottom panel: Simulation of frequency distribution of single cell
654 resistances in strain 7812, based on normal distribution curve fitting in panel B (top).

655



656

657 **Figure 2: Corroboration of inoculum effect assay for measurement of IC_{50} , heteroresistance and $\text{MIC}^{\text{MODEL}}$.**

658 Comparison of parameter determinations for randomly selected *Z. parabailii*, *Z. bailii* and *Z. pseudobailii*

659 isolates (isolates 7788, 7812, 7851, 7829, 7769, 7842). Values for IC_{50} (A), heteroresistance (B) and $\text{MIC}^{\text{MODEL}}$ (C)

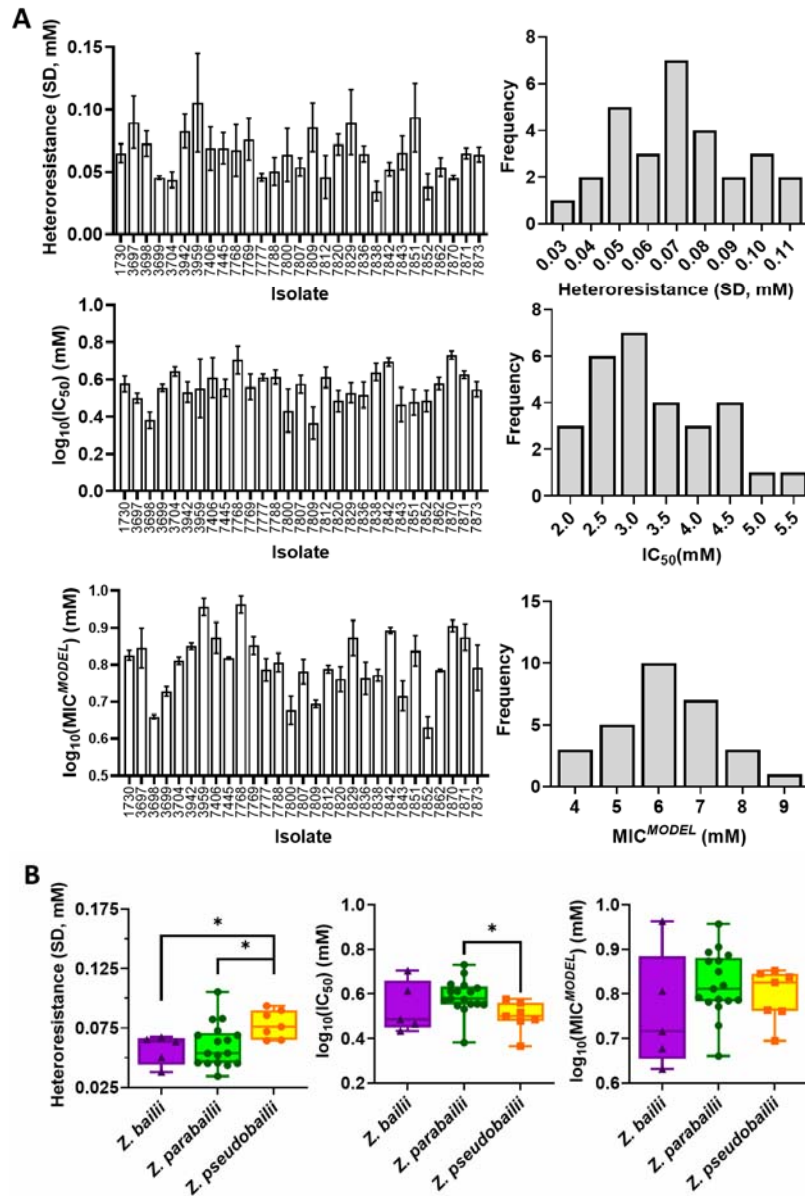
660 were derived either from dose-response curve on agar or inoculum effect assay in broth (using MIC^{EXP} values

661 at two inoculum sizes, see Methods). Points represent means from 6 biological replicates for each isolate +/-

662 SEM, with r values calculated using linear regression and p values were calculated using one-tailed linear

663 regression.

664



665

666

667

668 **Figure 3: Heteroresistance, IC_{50} and MIC^{MODEL} across a panel of 29 *Zygosaccharomyces* sp. isolates grown**
 669 **with sorbic acid. (A)** Left panels: heteroresistance, IC_{50} and MIC^{MODEL} determinations for individual strains.
 670 Values are means \pm SEM of average of parameters for three curves independently fitted to each biological
 671 replicate (MIC^{EXP} values measured at two inoculum sizes.) Right panels: Frequency histograms showing spread
 672 of heteroresistance, IC_{50} and MIC^{MODEL} in the 29-strain panel (strain list in Table 1). Values on the x axis indicate
 673 centre of each histogram bin, where divisions between bins were at the midpoints between adjacent values
 674 shown. **(B)** Data adapted from (A) to compare the distributions of heteroresistance, IC_{50} and MIC^{MODEL} among
 675 the isolates of the three subspecies. Significant differences are indicated (* $p < 0.05$), using two-sample *t*-test
 676 assuming unequal variances ($n = 5, 17$ and 7 , for *Z. bailii*, *Z. parabaillii* and *Z. pseudobailii*, respectively).

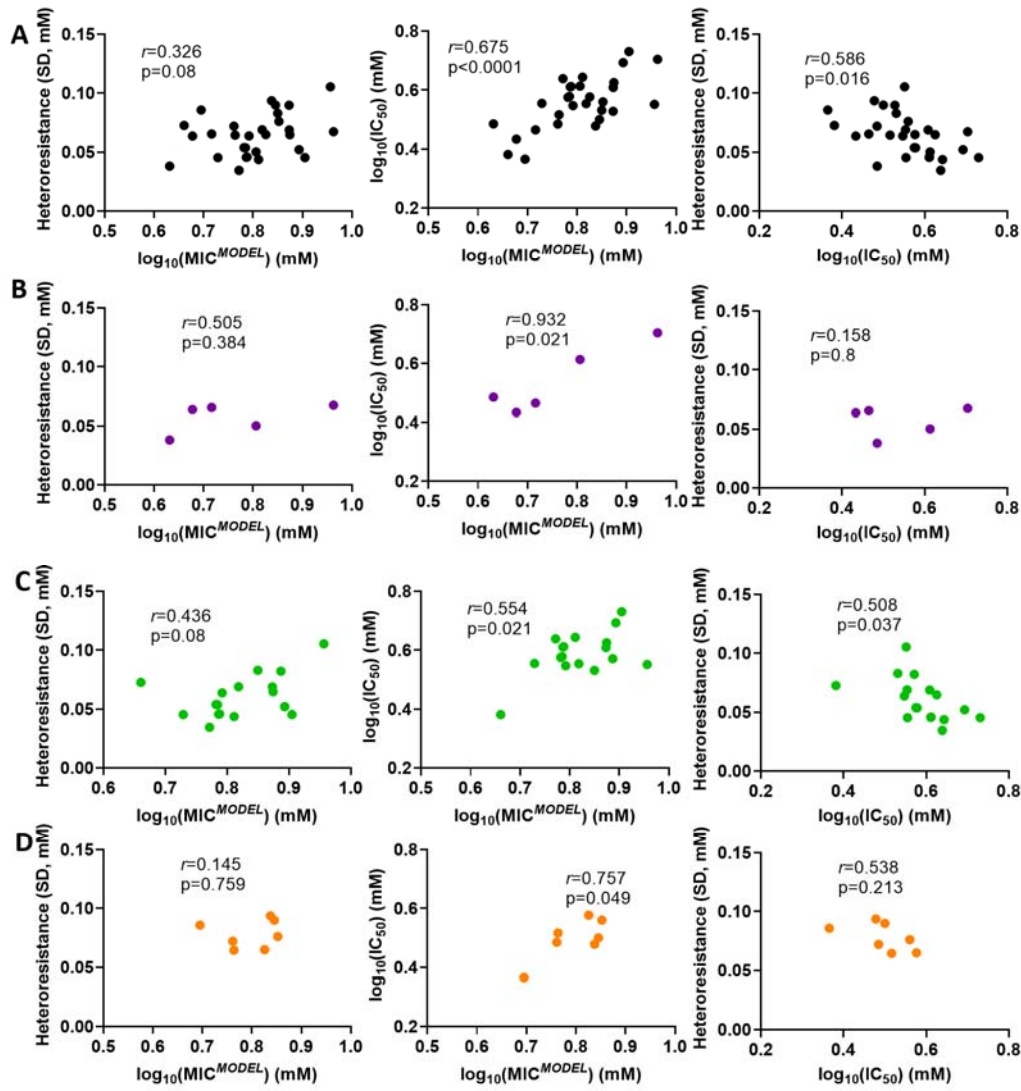
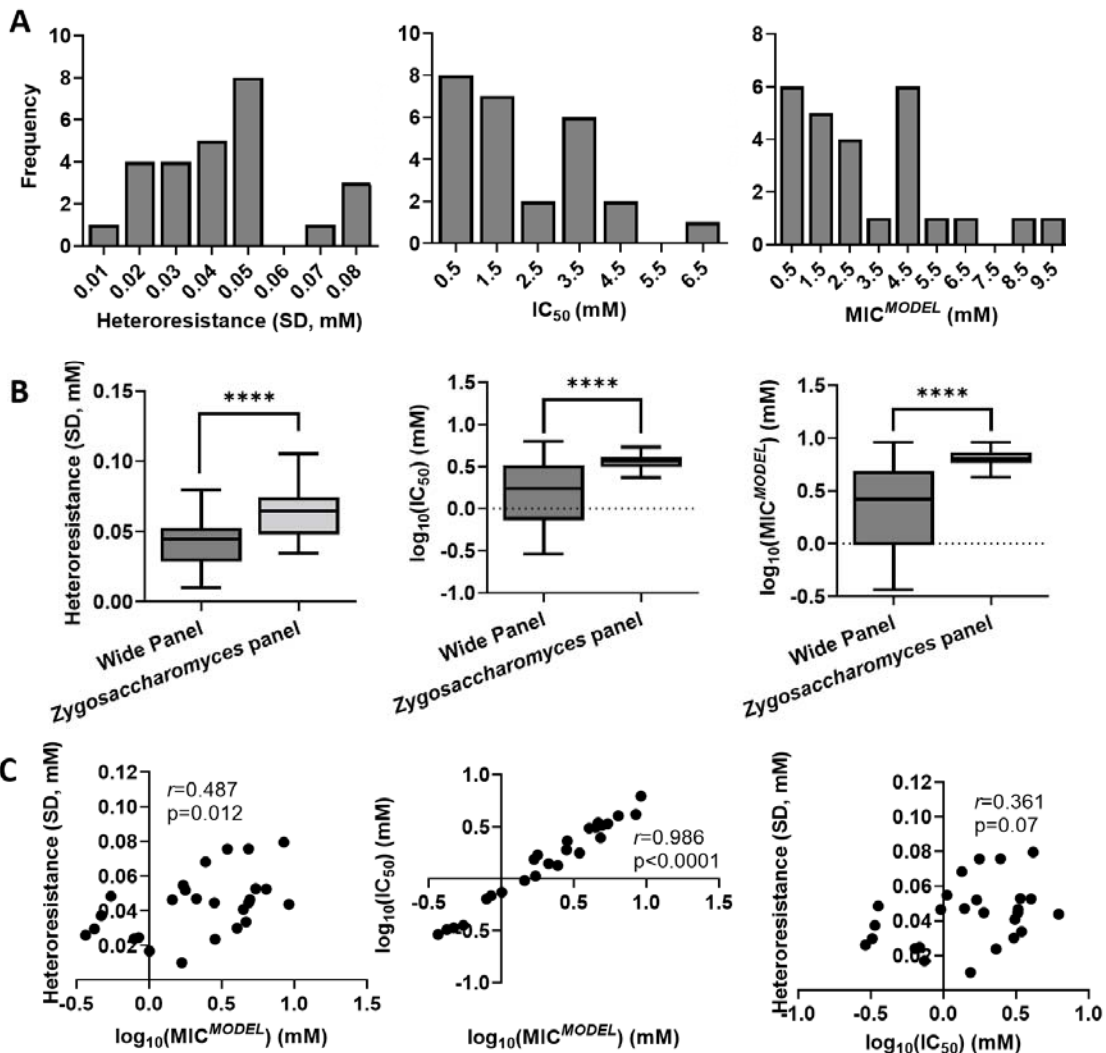


Figure 4: Relationships between heteroresistance, IC_{50} and MIC^{MODEL} in the main panel of *Zygosaccharomyces* sp. isolates. Data were obtained as described in Figure 3. (A) Cross-species panel of *Zygosaccharomyces* isolates (n=29) (Table 1). (B) *Z. bailii* only (n=5). (C) *Z. parabailii* only (n=17). (D) *Z. pseudobailii* only (n=7).

684



685

686

687

688 **Figure 5: Trends in sorbic acid heteroresistance, IC₅₀ and MIC^{MODEL} in a wide panel of diverse yeast species.**

689 **(A)** Frequency histograms showing the spread of heteroresistance, IC₅₀ and MIC^{MODEL} measured using the dose

690 response curve method. Values for individual 26 species are listed in Table S2. Values for individual isolates

691 were means from three biological replicates. **(B)** Box and whisker plots comparing the parameters between the

692 wide panel (n=26) and the *Zygosaccharomyces* panel (n=29) data from Figure 4. ***, p<0.0001 according to a

693 two-sample *t*-test assuming unequal variances. **(C)** Correlations between heteroresistance, IC₅₀ and MIC^{MODEL}

694 for the wide panel.

695